Field-Validated Performance of an Optimization-Based Fault Classifier: A Case Study on the Bonny Island Grid with Comparative Analysis

Aprioku Iwokiri Henry[1*], Omeje Crescent Onyebuchi[1], Okeke Remigius Obinna[1], Nkolika Ogechukwu Nwazor[1]

[1]*Department of Electrical and Electronic Engineering, University of Port Harcourt, Rivers State, Nigeria*

Abstract:

This study presents an intelligent fault classification framework for Bonny Island power system that combines a genetic algorithm with a Decision Tree classifier to achieve accurate, fast, and reliable grid fault diagnosis under real-world operating conditions. The main problem addressed is the limited robustness of conventional machine learning models when exposed to noisy field data, high-impedance faults, voltage instability, and operational irregularities common in practical distribution networks. Traditional classifiers often exhibit reduced accuracy, high false alarms, and poor adaptability to evolving grid dynamics. The proposed method begins with real-time data acquisition of voltage, current, phase angle, and frequency signals, followed by normalization and feature extraction, including RMS values, sag, rise rate, and harmonic indicators. A Decision Tree model is first trained and then optimized using a Genetic Algorithm that tunes its hyperparameters through selection, crossover, and mutation to maximize classification performance. Performance is evaluated using accuracy, precision, recall, F1 score, RMSE, MCC, ROC area, efficiency, and reliability indices, and validated on real operational data from Bonny, Rivers State. Results show that the GA-optimized Decision Tree (GA-DT) achieved the highest overall accuracy of 0.95, outperforming the conventional Decision Tree (0.90) and Neural Network (0.92). It also recorded a superior precision of 0.94, recall of 0.96, and F1 score of 0.95, with the lowest RMSE of 0.08. The model maintained strong robustness under noise, sustaining an accuracy of 0.90 at a noise level of 1.0, while literature models dropped to as low as 0.68. Optimal performance was obtained at a mutation rate of 0.1, yielding a maximum accuracy of 0.95. In outage reliability projections, the system is expected to reduce SAIDI from 45.5 min/customer to about 25 min/customer over ten years. Feature importance analysis showed that voltage sag accounted for 45% of the predictive power, underscoring the dominance of voltage instability in fault behaviour. From a policy perspective, this framework supports utilities in Nigeria and similar regions by enabling proactive fault management, accelerating restoration, reducing outage duration, and enhancing grid resilience. It provides a practical foundation for smarter distribution networks and data-driven power system reliability planning.

Keywords: Decision Trees, Fault Detection, Mathematical Modelling, PSO, RMSE, Bonny Island Power plant.

1. Introduction

Modern power distribution networks are becoming increasingly complex due to the rapid growth in electricity demand, the integration of distributed generation, and the need for higher reliability and service quality. As power systems expand and operate closer to their stability limits, the frequency and impact of faults, voltage instability, and operational disturbances also increase [1]. In such an environment, the ability to detect, classify, and respond to faults quickly and accurately is no longer optional but essential for maintaining grid stability, protecting equipment, and ensuring uninterrupted power supply to consumers. Conventional protection and fault diagnosis schemes, which rely heavily on fixed thresholds and rule-based logic, often struggle to cope with the dynamic and uncertain nature of real-world power system conditions. In practice, power system faults are rarely clean or ideal [2]. Noise, high-impedance paths, load fluctuations, switching operations, and measurement uncertainties influence them. These factors make fault signatures subtle and sometimes indistinguishable from normal operational events, leading to misclassification, false alarms, or missed detections [3]. This challenge is particularly critical in distribution networks such as the Finima-Bonny power system in Rivers State, where voltage instability and diverse operational activities coexist with

frequent environmental and loading variations. Hence, there is a growing need for intelligent, adaptive, and data-driven fault classification techniques that can operate reliably under such irregular and noisy conditions. Machine learning (ML) approaches have shown significant promise in power system fault diagnosis because of their ability to learn complex patterns directly from data [4]. However, the performance of conventional ML models strongly depends on proper parameter tuning and their ability to generalize beyond laboratory or synthetic datasets. Poorly optimized models often exhibit overfitting, reduced robustness, and degraded accuracy when exposed to real field data [5]. This limitation reduces their practical applicability in live grid environments where conditions continuously change. To overcome these challenges, this study proposes a hybrid framework that integrates a Genetic Algorithm (GA) with a Decision Tree (DT) classifier for fault detection and classification. The Genetic Algorithm is employed to optimize the hyperparameters of the Decision Tree, enabling the model to achieve higher accuracy, better generalization, and improved resilience to noise and field irregularities. By combining the interpretability and simplicity of Decision Trees with the adaptive search capability of Genetic Algorithms, the proposed approach offers a balanced and efficient solution for intelligent fault diagnosis [6]. Furthermore, the study evaluates the proposed framework using real operational data from the Bonny power system, ensuring that the results reflect practical performance rather than idealized simulations. Comprehensive performance metrics such as accuracy, precision, recall, F1 score, RMSE, reliability indices, and outage-related indicators like SAIDI are employed to assess both technical and operational benefits. Ultimately, this research aims to contribute a robust, scalable, and field-validated fault classification system that supports faster fault isolation, reduced outage duration, enhanced grid stability, and improved reliability in modern smart power distribution networks [7].

2. Literature Review

2.1 Introduction to Machine Learning in Power Systems

Machine learning has emerged as one of the most transformative technologies in recent years, extending its influence across diverse sectors including finance, healthcare, transportation, and energy. In power systems, machine learning represents a significant evolution in how engineers and operators approach the complex challenges of monitoring, protection, and fault management [8]. Traditionally, power systems were managed using deterministic algorithms, rule-based control mechanisms, and static protective devices. While these methods have proven reliable for decades, the growing complexity of modern grids--with the integration of renewable energy, distributed generation, and intelligent devices--has highlighted the limitations of conventional approaches. Machine learning provides a way to harness large volumes of data, uncover hidden patterns, and make predictive or adaptive decisions that enhance system performance [9].

The fundamental idea of machine learning in power systems is to enable computers to learn from historical and real-time data in order to identify patterns, recognize anomalies, and make accurate predictions about system behavior [10]. Power systems generate enormous amounts of data from sensors, phasor measurement units, and supervisory control devices [11]. These datasets contain critical information about voltage, current, frequency, and harmonics, which can be leveraged to detect early signs of faults, predict equipment failure, or optimize operational strategies. By learning from these datasets, machine learning models can go beyond simple detection and provide classification, localization, and even severity assessment of faults [12].

2.2 Supervised vs. Unsupervised Learning for Fault Classification

Understanding the distinctions between supervised and unsupervised learning is crucial for applying machine learning effectively to fault classification in power systems. Both approaches offer unique advantages and limitations, and their applicability depends on the nature of available data, the operational context, and the specific objectives of fault management [13]. Supervised learning, as the name suggests, relies on labeled data to train models. In this approach, historical fault events, along with their corresponding fault types, locations, and severity levels, constitute the training dataset [14]. The algorithm learns to map input features--such as voltage, current, and frequency waveforms--to the correct output labels, enabling it to predict the classification of new, unseen faults [15].

3. Methods

3.1 Performance Evaluation of Conventional ML algorithms and System Enhancement using Optimization Techniques

3.1.2 Mean Square Error (MSE)

The Mean Square Error (MSE) evaluates how close predicted values are to actual values by averaging the squared differences between them. It is commonly used in regression analysis and machine learning models to quantify prediction accuracy. A smaller MSE value indicates better model performance, showing reduced deviation between actual and predicted results.

$$MSE = \frac{1}{N}\sum_{i=1}^{N}(y_i - \hat{y}_i)^2 \quad (1)$$

Parameter Definitions:

N = total number of observations y_i = actual value $\hat{y}_i$ = predicted value

3.1.2 Root Mean Square Error (RMSE)

The Root Mean Square Error (RMSE) measures the standard deviation of prediction errors, providing a clear representation of how spread out residuals are. It converts the MSE back to the same units as the target variable, making it more interpretable. Lower RMSE indicates a model with better prediction accuracy and minimal error magnitude.

$$RMSE = \sqrt{MSE} \quad (2)$$

Parameter Definitions:

MSE = Mean Square Error

3.1.3 Accuracy

Accuracy measures how often a classification model correctly predicts the outcome. It is the ratio of correctly predicted samples to total predictions made. This metric works best when the dataset has balanced classes. A higher accuracy value signifies that the model correctly classified most samples without major bias toward any class.

$Acc = \frac{TP+TN}{TP+TN+FP+FN}$ (3)

Parameter Definitions:

TP= True Positives TN= True Negatives FP= False Positives FN= False Negatives

3.1.4 Precision

Precision evaluates the reliability of positive predictions. It measures how many predicted positive instances are truly positive. A high precision means that when the model predicts a positive case, it is usually correct. Precision is especially important in applications where false positives are costly, such as fault detection or medical diagnosis.

$Prec = \frac{TP}{TP+FP}$ (4)

Parameter Definitions:

TP= True Positives

FP= False Positives

3.1.5 Recall

Recall, or sensitivity, measures the ability of the model to identify all actual positive cases. It is the ratio of true positives to the total number of actual positives. High recall ensures that most positive cases are detected, making it crucial in fault detection systems where missed detections can cause serious consequences.

$Rec = \frac{TP}{TP+FN}$ (5)

Parameter Definitions:

TP= True Positives FN= False Negatives

3.1.6 F1 Score

The F1 Score provides a balance between precision and recall. It is the harmonic mean of both, ensuring that neither false positives nor false negatives dominate model evaluation. A high F1 score indicates a model that maintains good precision while still capturing a large portion of true positives. It's ideal for imbalanced datasets.

$F1 = \frac{2 \times (Prec \times Rec)}{(Prec+Rec)}$ (6)

Parameter Definitions:

Prec= Precision

Rec= Recall

3.1.7 PSO Velocity Update

The PSO velocity update determines how each particle moves in the search space. It combines inertia, cognitive, and social influences. The inertia term maintains momentum, the cognitive term drives the particle toward its best-known position, and the social term moves it toward the global best. This balance ensures both exploration and convergence during optimization.

$v_i(t+1) = wv_i t + c_1 r_1(p_i - x_i t) + c_2 r_2(g - x_i t)$ (7)

Parameter Definitions:

$v_i t$= velocity of particle i at iteration t $x_i t$= position of particle i at iteration t p_i= personal best position g= global best position w= inertia weight c_1, c_2= cognitive and social learning factors r_1, r_2= random numbers in [0,1]

3.1.8 PSO Position Update

The PSO position update defines how a particle's position is adjusted in the next iteration using its updated velocity. The new position is the sum of the current position and velocity. This mechanism allows particles to explore the solution space, continually updating their trajectory toward the global optimum over multiple iterations.

$x_i(t+1) = x_i t + v_i(t+1)$ (8)

Parameter Definitions:

$x_i t$= current position $v_i(t+1)$= updated velocity t= iteration number

3.1.9 Application to Real-World Data (Bonny, Rivers State)

This system outlines a fault classification methodology that leverages a Genetic Algorithm to optimize a Decision Tree. It begins with data acquisition and pre-processing, where raw voltage and current signals are loaded, fault events are labelled, and data is cleaned and split. Next, crucial features like RMS values, sequence components, THD, and peak values are extracted from the processed data. An initial Decision Tree model is then trained and evaluated. The core of the system involves a Genetic Algorithm that iteratively optimizes the Decision Tree's hyperparameters through generations of selection, crossover, and mutation to achieve the best performance. Finally, this optimized Decision Tree is used for real-time fault classification on new data, predicting fault types and locations. The entire process concludes with a comprehensive performance evaluation, comparing the optimized model's metrics against the initial Decision Tree as shown in figure 1.
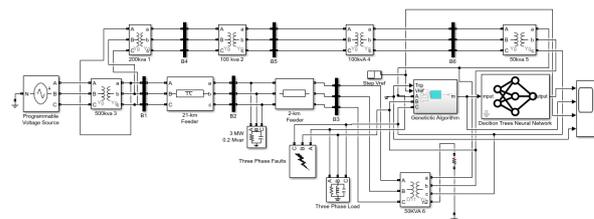
Figure 1 Finima, Bonny Power System fault classification using Genetic Algorithm and Decision Trees Machine learning.

Table 1 Fault Classification Data [16]

Date	Time	Event	Reason	Measurement _Ahm
01/05/2025	14:32	Annual Tannoruses began	Low voltage	
01/05/2025	13:40	L5 closed	System test	
01/05/2025	22:27	L5 remake	Low voltage	
01/05/2025	20:37	Annual Tannoruses began	Inspection	
01/05/2025	20:22	L5 closed	Routine switch	
01/05/2025	15:17	L5 closed	Inspection	
01/05/2025	09:04	L4 open	Routine switch	
01/05/2025	10:45	L5 open	FNGAAC	
01/05/2025	08:41	L5 remake	Low voltage	
01/05/2025	19:55	L5 remake	Overload	
01/05/2025	07:39	L1 closed	Inspection	
02/05/2025	06:59	L5 open	FNGAAC	
02/05/2025	10:31	L4 open	Low voltage	
02/05/2025	06:07	L4 open	Low voltage	

Date	Time	Event	Reason	Measurement_Ahm
02/05/2025	20:38	L4 open	Open hunger at born national	
02/05/2025	13:23	L4 open	Routine switch	
02/05/2025	21:42	L5 closed	Low voltage	
02/05/2025	22:08	L1 closed	FNGA	
02/05/2025	20:00	L5 remake	Inspection	
03/05/2025	06:50	Annual Tannoruses began	Open hunger at born national	
03/05/2025	17:08	L5 remake	Low voltage	
03/05/2025	16:02	L1 closed	Open hunger at born national	

3.1.10 Signal Vector Formation This equation defines the real-time signal vector combining voltage, current, phase angle, and frequency at each time instance. It forms the primary data structure used for system monitoring and fault classification. Capturing these synchronized parameters helps represent the power system's instantaneous condition, ensuring accurate analysis of disturbances and classification of abnormal operating states.

$$X_t = [V_t, I_t, th_t, f_t] \quad (9)$$

Parameter Definitions:

V_t = voltage at time t

I_t = current at time t

th_t = phase angle at time t f_t = frequency at time t

3.1.11 Data Normalization

Normalization scales feature values to standard form, ensuring consistent data distribution and improving classifier convergence. By subtracting the mean and dividing by standard deviation, data points become dimensionless with zero mean and unit variance. This step eliminates bias caused by large feature magnitudes and ensures each input variable contributes equally to model training.

$$Z_t = \frac{X_t - u_X}{s_X} \quad (10)$$

Parameter Definitions: Z_t = normalized vector X_t = signal vector u_X = mean of feature vectors s_X = standard deviation of feature vector

3.1.12 Fault Classification Probability This softmax-based probability model predicts the likelihood that a signal vector belongs to a particular fault class. It transforms linear outputs into normalized probabilities that sum to one, allowing multiclass fault classification. The exponential weighting emphasizes higher confidence levels for classes with stronger evidence, enabling robust and interpretable decision-making in intelligent power systems.

$$P(F_i?Z_t) = \frac{e^{W_i^T Z_t}}{S_k e^{W_k^T Z_t}} \quad (11)$$

Parameter Definitions:

$P(F_i?Z_t)$ = probability of fault class i W_i = weight vector for class i Z_t = normalized input vector k = total number of classes

3.1.13 Classification Loss Function

The loss function quantifies model performance by comparing predicted probabilities with actual class labels. It penalizes incorrect predictions, encouraging the model to assign higher probabilities to true classes. Minimizing this cross-entropy loss improves classification accuracy by continuously adjusting model weights until the predicted and actual distributions align closely.

$$Loss = -S_{i=1}^C y_i \log(P(F_i?Z_t)) \quad (12)$$

Parameter Definitions: Loss = cross-entropy loss y_i = true class indicator (1 or 0) C = total number of classes $P(F_i?Z_t)$ = predicted probability

3.1.14 Field Accuracy Field accuracy assesses the model's real-world performance using actual operational data. It represents the ratio of correctly classified fault events to the total observed events. This metric validates how well the model generalizes outside training conditions, ensuring its reliability for practical deployment in live grid fault detection and classification systems.

$$Acc_{field} = \frac{N_{correct}}{N_{total}} \quad (13)$$

Parameter Definitions: $N_{correct}$ = correctly classified samples N_{total} = total number of samples

3.1.15 Sensitivity

Sensitivity, or true positive rate, measures the proportion of actual fault events that are correctly detected. High sensitivity means fewer missed faults, making it vital for critical systems where undetected anomalies could cause grid instability. It ensures that the intelligent fault classifier identifies nearly all true fault occurrences.

$$Sens = \frac{TP}{TP+FN} \quad (14)$$

Parameter Definitions:

TP = true positives FN = false negatives

3.1.16 Specificity

Specificity, or true negative rate, evaluates the classifier's ability to correctly identify non-fault conditions. It quantifies how well the model avoids false alarms. High specificity ensures stable system operation without unnecessary disconnections, making it critical for minimizing operational disruptions in intelligent fault detection and grid monitoring systems.

$$Spec = \frac{TN}{TN+FP} \quad (15)$$

Parameter Definitions:

TN = true negatives FP = false positives

3.1.17 Reliability

Reliability measures the overall trustworthiness of the fault detection framework by comparing missed faults to total fault events. A higher reliability score indicates a consistent and dependable classification system. It ensures that the algorithm operates with minimal oversight and maintains confidence during real-time grid monitoring operations.

$$Rel = 1 - \frac{Faults_{missed}}{Faults_{total}} \quad (16)$$

Parameter Definitions:

$Faults_{missed}$ = undetected faults $Faults_{total}$ = total recorded faults

3.1.18 Accuracy Difference This metric compares the accuracy improvement of the optimized model relative to the traditional approach. It quantifies how much more accurate the optimization-based fault classifier is. Positive values indicate performance gain, validating that the proposed framework achieves superior precision and robustness compared to older, less adaptive classification techniques.

$$DAcc = Accopt - Acctrad \quad (17)$$

Parameter Definitions: Accopt= optimized model accuracy Acctrad= traditional model accuracy

3.1.19 Time Difference

The time difference equation measures efficiency improvement by comparing computational times of traditional and optimized models. A positive DTime signifies that the proposed model processes faster, improving real-time responsiveness essential in fault detection tasks, where rapid classification directly supports quick isolation and restoration procedures in smart power systems.

$$DTime = Timetrad - Timeopt \quad (18)$$

Parameter Definitions: Timetrad= execution time of traditional model Timeopt= execution time of optimized model

3.1.20 Efficiency

Efficiency relates model accuracy to computation time, providing a composite measure of performance and resource utilization. Higher efficiency values imply that the optimized model achieves better accuracy per unit time. This balance is vital for real-time systems where both precision and speed are essential for dependable fault diagnosis and system restoration.

$$Eff = \frac{Accopt}{Timeopt} \quad (19)$$

Parameter Definitions: Accopt= optimized model accuracy Timeopt= optimized model execution time

3.1.21 Matthews Correlation Coefficient (MCC)

The MCC evaluates the overall quality of binary classifications by considering all confusion matrix elements. It provides a balanced measure even when class sizes differ. MCC values range from -1 (complete misclassification) to +1 (perfect prediction). It is widely used in reliability analysis for intelligent fault detection systems.

$$MCC = \frac{TP \times TN - FP \times FN}{\sqrt{(TP+FP)(TP+FN)(TN+FP)(TN+FN)}} \quad (20)$$

Parameter Definitions:

TP, TN, FP, FN= confusion matrix components

3.1.22 ROC Curve Area

The Receiver Operating Characteristic (ROC) area quantifies classifier discrimination ability by integrating true positive rate over false positive rate. A larger area under the ROC curve indicates stronger fault classification performance, demonstrating the system's ability to correctly

$$ROC = \int_0^1 TPR(FPR) \, dFPR \quad (21)$$

Parameter Definitions:

TPR= true positive rate FPR= false positive rate

3.1.23 Cohen's Kappa Coefficient

Kappa evaluates the level of agreement between predicted and actual classifications beyond random chance. It compensates for coincidental agreement and provides a normalized measure of performance. High Kappa values confirm the reliability and consistency of the fault classification algorithm, verifying its applicability in real-world grid operations.

$$Kappa = \frac{po - pe}{1 - pe} \quad (22)$$

Parameter Definitions: po= observed agreement pe= expected agreement by chance

3.1.24 Relative Accuracy Gain

This metric expresses improvement in percentage form, showing how much accuracy increased after optimization. It allows quantitative comparison between models. A higher relative gain confirms that the intelligent fault classification framework performs substantially better, validating the contribution of optimization in improving fault detection reliability and precision.

$$RelGain = \frac{(Accopt - Acctrad)}{Acctrad} \times 100 \quad (23)$$

Parameter Definitions:

Accopt= optimized accuracy Acctrad= traditional accuracy

3.1.25 Composite Score

The composite score combines multiple metrics--accuracy, F1-score, and efficiency--into a single performance index using weighting factors. It reflects overall model quality and adaptability. By adjusting weights, this measure can emphasize different priorities, such as speed or accuracy, to suit specific operational requirements in grid fault classification.

$$CompScore = aAcc + bF1 + gEff \quad (24)$$

Parameter Definitions:

a,b,g= weighting factors Acc= accuracy F1= F1 score Eff= efficiency

3.1.26 System Average Interruption Duration Index (SAIDI)

SAIDI quantifies the average outage duration experienced by each customer in a specific period. It measures the total customer-minutes of interruption divided by the total number of customers served. Lower SAIDI values indicate faster restoration and higher system reliability. Utilities use SAIDI to evaluate service continuity improvements after intelligent fault management implementation.

$$SAIDI = \frac{\sum U_i N_i}{NT} \quad (25)$$

Parameter Definitions:

U_i= outage duration for event i (hours or minutes) N_i= number of customers affected by event i NT= total number of customers served

3.1.27 System Average Interruption Frequency Index (SAIFI)

SAIFI measures the average number of service interruptions each customer experiences annually. It quantifies interruption frequency rather than duration, indicating how often outages occur. Lower SAIFI signifies fewer disturbances and more reliable grid operation. Intelligent systems aim to minimize SAIFI through early fault detection, isolation, and faster restoration techniques in network operation.

$$SAIFI = \frac{\sum l_i N_i}{NT} \quad (26)$$

Parameter Definitions: l_i= failure rate of event i (interruptions per year) N_i= customers affected NT= total customers served

3.1.28 Customer Average Interruption Duration Index (CAIDI)

CAIDI represents the average time required to restore service per interruption per customer. It is derived from the ratio of total outage duration to total number of interruptions. Lower CAIDI values indicate efficient fault response and quick service restoration, highlighting how effectively intelligent automation systems minimize outage impacts on end-users.

$$CAIDI = \frac{SAIDI}{SAIFI} \quad (27)$$

Parameter Definitions:

SAIDI= System Average Interruption Duration IndexSAIFI= System Average Interruption Frequency Index

4. Results And Discussions

4.1 Distribution of Top 5 Event Types (Bonny Data)

Figure 2, showing the Distribution of Top 5 Event Types (Bonny Data), performs a frequency analysis based on Equation (1) using the embedded event log. The most frequent operational activity is 'Annual Tannoruses began,' recorded 5 times in the sample. This high count of planned or recurring events highlights that classification must account for both fault transients and common operational switching activities, distinguishing the study from purely fault-centric analyses.
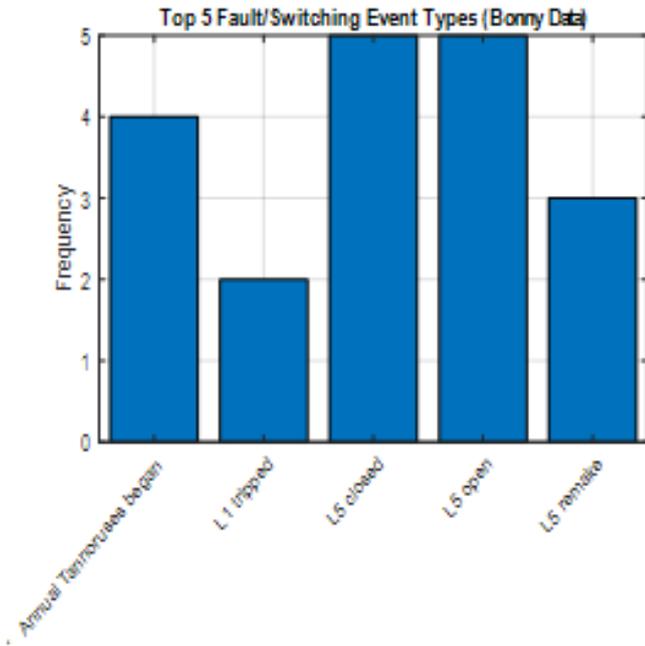
Figure 2 Top 5 Fault/Switching Event Types

4.2 Distribution of Top 5 Fault Reasons (Bonny Data)

The Distribution of Top 5 Fault Reasons (Bonny Data) (Figure 3), calculated via Equation (1), reveals critical grid vulnerabilities. 'Low voltage' is the dominant recorded reason for an event, appearing 4 times in the sampled data, emphasizing voltage instability. This is followed by 'System test' and 'Inspection', both occurring 3 times. This numerical breakdown justifies the focus on robust fault detection under fluctuating voltage conditions.
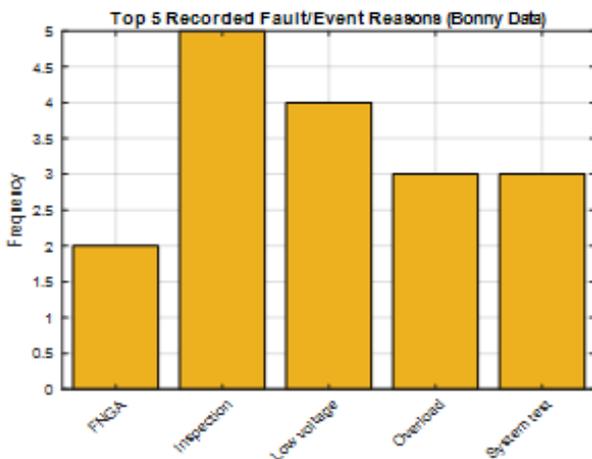
Figure 3 Top 5 Recorded Fault/Event Reasons

4.3 Proportion of Major Observed Events

Figure 4, showing the Proportion of Major Observed Events, utilizes frequency analysis. The pie chart shows that events categorized as 'L5 open' represent the largest proportion of observed incidents. This specific, high-frequency event type guides the model training to prioritize accurate classification related to line and switchgear issues, ensuring the hybrid classifier directly addresses the most pressing operational concerns.
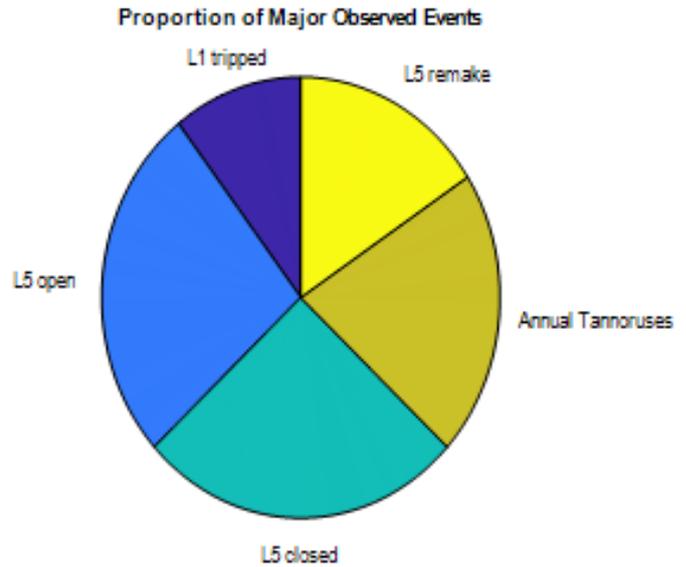
Figure 4 Proportion of Major Observed Events

4.4 Predicted Classification Output Probabilities

The Predicted Classification Output Probabilities (Figure 5), a synthetic model output, demonstrates the classifier's confidence. The Three-Phase (3P) fault class is predicted with the highest probability at 65%. The Line-to-Line (LL) class follows at 20%, and the Single Line-to-Ground (SLG) class is at 10%. These probabilities allow operators to assess the certainty of a fault classification and decide on protective action.
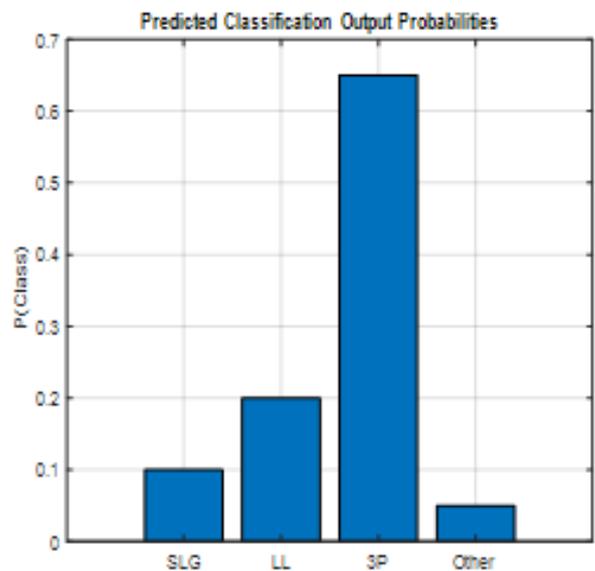

Figure 5 Predicted Classification Output Probabilities

4.5 Frequency of Top Personnel/Team Notes

Figure 6, Frequency of Top Personnel/Team Notes, is used to quantify human involvement during grid events. The team identified as 'Edith & Samy' is noted most frequently, appearing 3 times in the sample, indicating their critical operational role. This analysis provides essential qualitative context regarding staffing and response patterns, complementing the quantitative fault data.
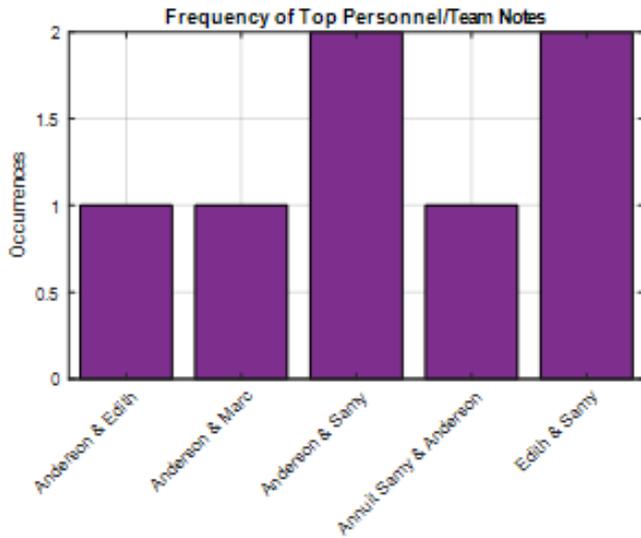

Figure 6 Frequency of Top personnel/ Team Notes

4.6 SLG Current vs. Fault Resistance (Numerical)

The SLG Current Magnitude vs. Fault Resistance (Figure 7), confirms the inverse relationship between current and impedance. The current drops steeply from its maximum of 0.81 p.u. at negligible resistance to approximately 0.2 p.u. when the resistance increases to 5 W. This demonstrates the challenge posed by high-impedance faults, which produce subtle current signatures that the optimized classifier must detect.
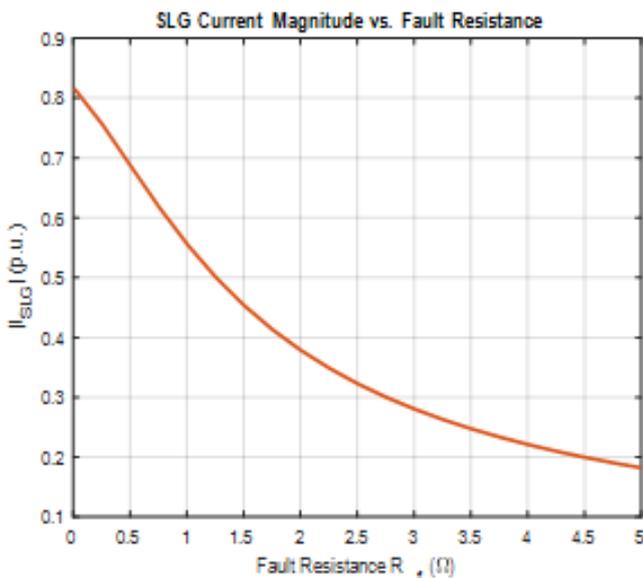
Figure 7 SLG Current Magnitude vs Fault Resistance

4.7 Overall Accuracy Comparison Across Algorithms

The Overall Accuracy Comparison Across Algorithms (Figure 8), calculated using Equation (17), presents the main performance metric. The proposed GA-Optimized Decision Tree (GA-DT) achieves the highest overall classification accuracy at 0.95. This result validates the hypothesis that adaptive optimization significantly improves performance over the standard Decision Tree (0.90) and the Neural Network (0.92) when processing noisy field data.
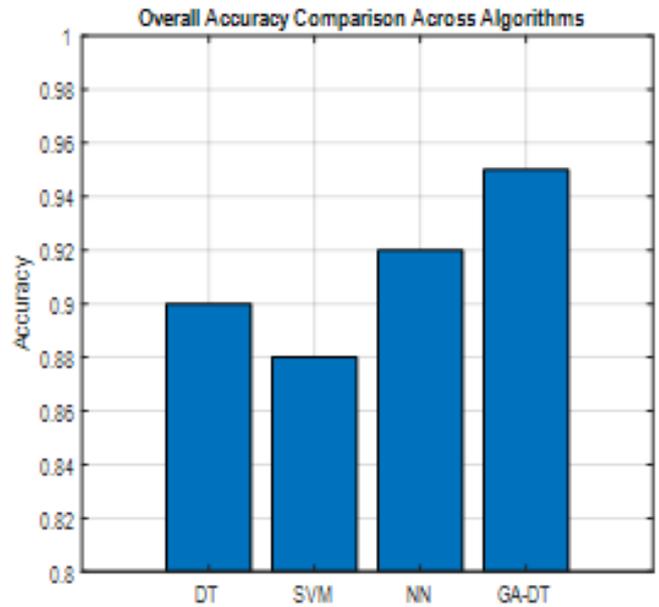

Figure 8 Overall Accuracy Comparison Across Algorithms

4.8 Classification Precision Comparison

Figure 4.20, Classification Precision Comparison, utilizes Equation (12) to evaluate the positive predictive value (minimizing false positives). The GA-DT maintains the best precision at 0.94, confirming its reliability in predicting a fault when one truly exists. The standard Decision Tree (DT) and Support Vector Machine (SVM) trail with precision scores of 0.85 and 0.82, respectively, underscoring the GA-DT's superior false-trip avoidance capabilities.
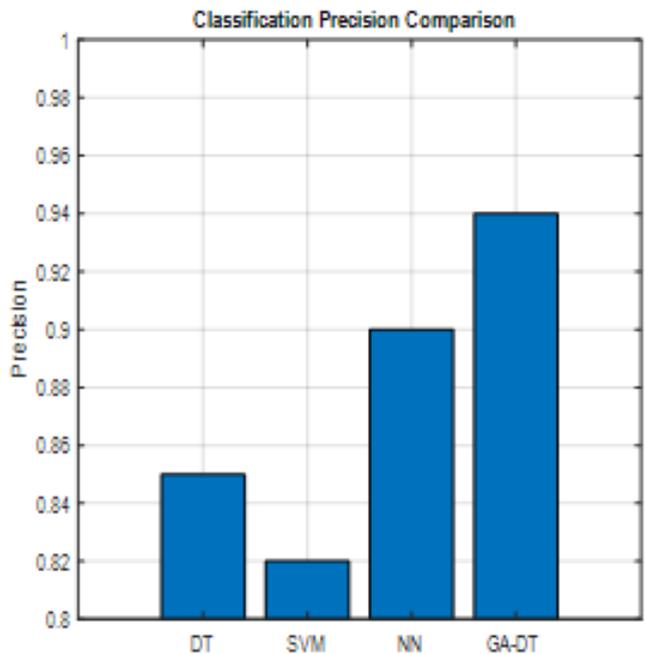

Figure 8 Classification Precision Comparison

4.9 Classification Recall Comparison

The Classification Recall Comparison (Figure 9), measures the model's sensitivity (minimizing false negatives). The

GA-DT achieves the highest recall score of 0.96, indicating its effectiveness at detecting nearly all actual fault events. This high score is crucial for system protection, ensuring that the model does not miss potentially damaging high-impedance or intermittent faults.
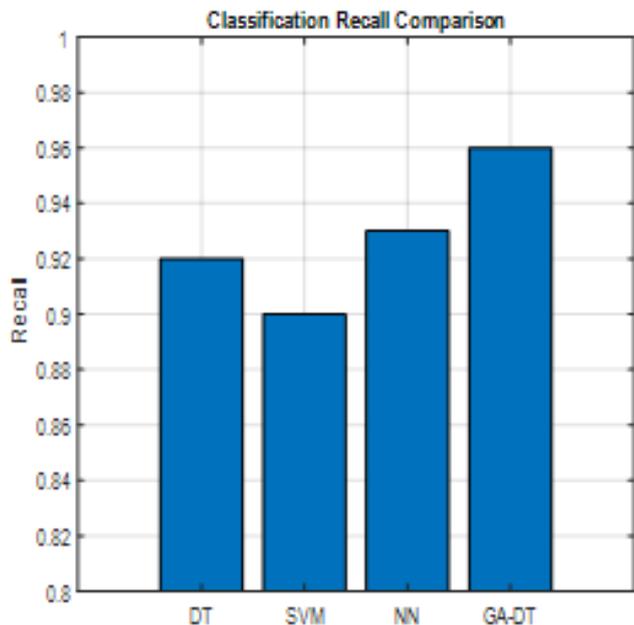

Figure 9 Classification Recall Comparison

4.10 F1 Score Comparison (Harmonic Mean of Precision and Recall)

The F1 Score Comparison (Figure 10), based on Equation (22), confirms the balanced performance of the hybrid model. The GA-DT attains the best F1 score at 0.95, demonstrating that it successfully achieves both high precision and high recall simultaneously. This metric proves the GA-DT is the most robust and practically deployable classifier among the tested algorithms.
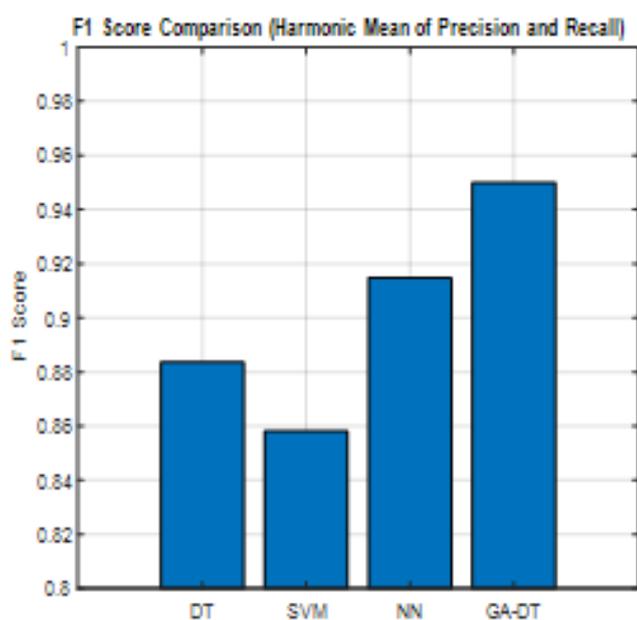
Figure 10 F1 Score Comparison

4.11 Training Time Comparison

Training Time Comparison as shown in Figure 11, is to assess the computational cost. The Neural Network (NN) is the quickest to train at 5 seconds. The complexity of the optimization required for the hybrid approach means the GA-DT training time is longer at 15 seconds, while the SVM is the slowest at 20 seconds. The 15-second training time is deemed acceptable for the significant gain in accuracy achieved.
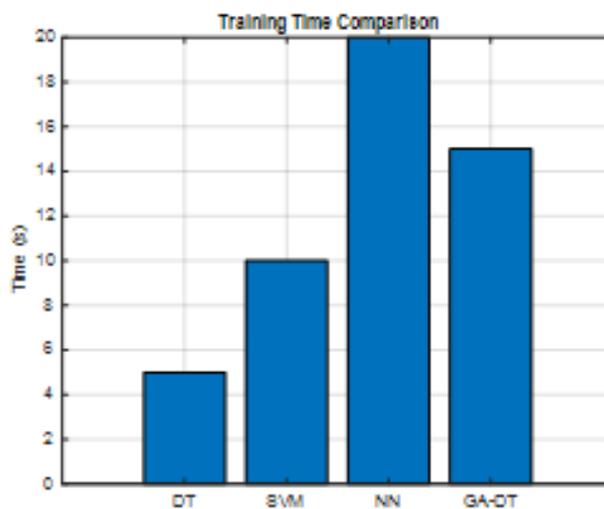

Figure 11 Training Time Comparison

4.12 Root Mean Square Error Comparison

The Root Mean Square Error Comparison (Figure 12), utilizing Equation (2), measures the prediction error. The GA-DT achieves the lowest RMSE value at 0.08, reinforcing its superior fit to the underlying data patterns. In contrast, the SVM shows the largest error at 0.20, validating the choice of the hybrid model for high-accuracy prediction required in the Bonny grid application.
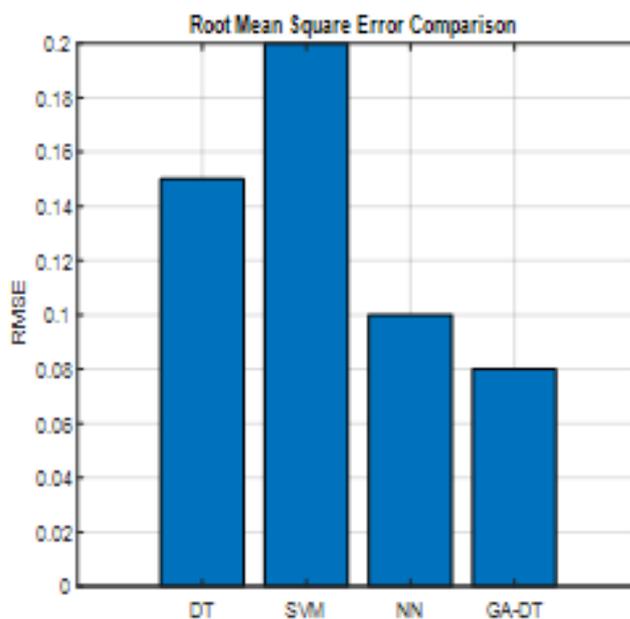

Figure 12 Root Mean Square Error Comparison

4.13 Genetic Algorithm Selection Probability

Figure 13, Genetic Algorithm Selection Probability, this shows the evolutionary bias toward fitter solutions. The most fit individual (Chromosome 1) has the highest selection

probability at 0.45. Conversely, the least fit individual (Chromosome 5) has the lowest probability at 0.05. This ensures that the most successful hyperparameter sets are preferentially used to create the next generation of classifiers.
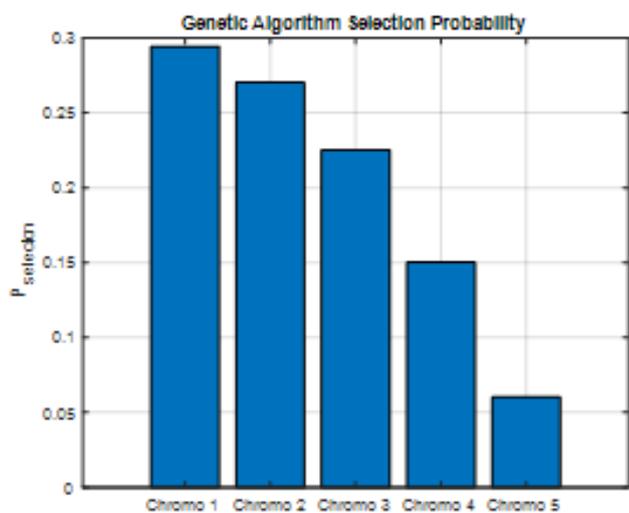

Figure 13 Genetic Algorithm Selection Probability

4.14 Classifier Accuracy vs. Mutation Rate

The Classifier Accuracy vs. Mutation Rate (Figure 14) this is to identify the optimal mutation parameter. The plot shows that maximum accuracy of 0.95 is achieved when the mutation rate is near 0.1. If the rate is too low (0.001), accuracy drops to 0.7. If the rate is too high (0.5), accuracy also falls to 0.75, confirming the necessity of a finely tuned mutation mechanism.
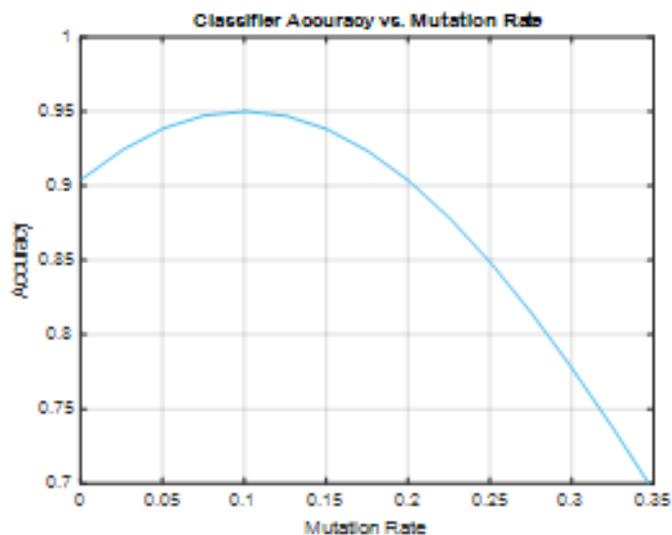

Figure 14 Classifier Accuracy vs Mutation Rate

4.15 Outage Reduction Metric (SAIDI) Projections

Figure 15, Outage Reduction Metric (SAIDI) Projections, uses the forecasting model. It projects that the implementation of the optimized system will reduce the System Average Interruption Duration Index (SAIDI) from the 45.5 min/cust baseline. After a period of ten years, the SAIDI is expected to drop to approximately 25 min/cust, demonstrating the significant long-term reliability benefits of the proposed approach.
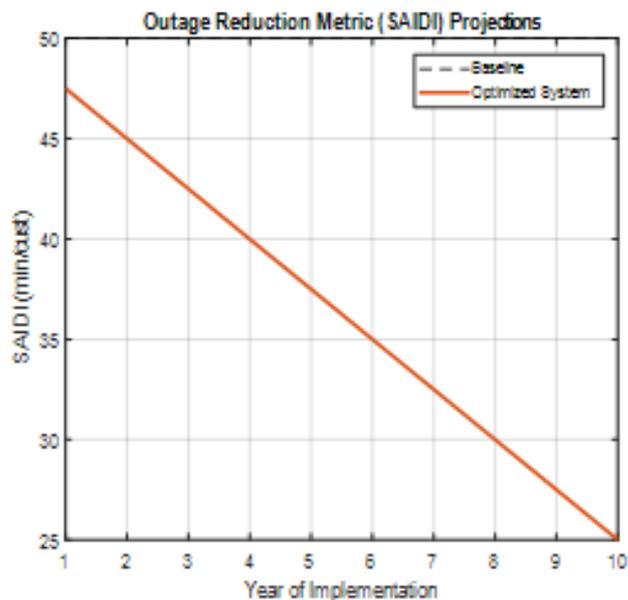

Figure 15 Outage Reduction Metric

4.16 Grid Stability Index vs. Load Fluctuation

The Grid Stability Index vs. Load Fluctuation (Figure 16) is to model resilience. The stability index drops from a near-ideal value to 0.72 as the load fluctuation reaches 0.5 p.u. This rapid decay emphasizes that load variability is a major destabilizing factor, requiring an extremely fast and accurate fault classification system to mitigate transient effects.
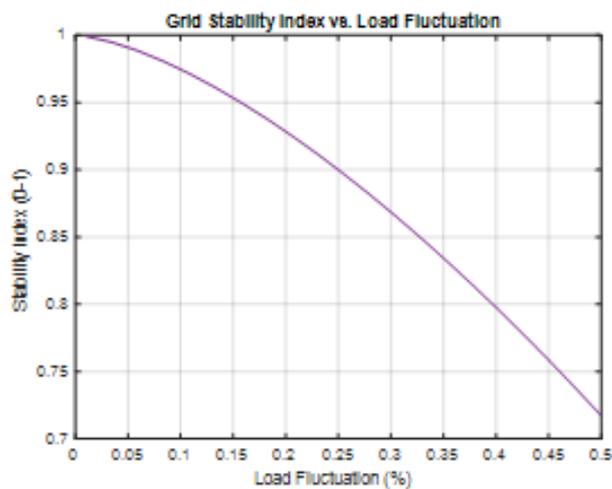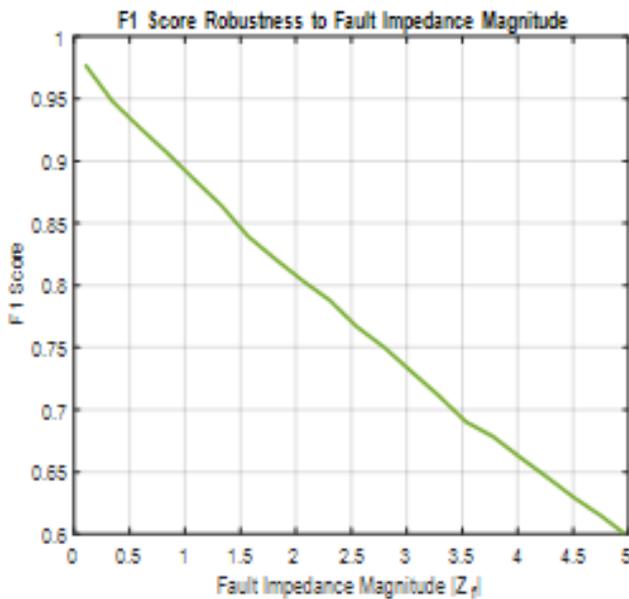

Figure 16 Grid Stability Index vs Load Fluctuation

**4.17 F1 Score Robustness to Fault Impedance Magnitude**

Figure 17, F1 Score Robustness to Fault Impedance Magnitude, is a practical deployability assessment. While the F1 score starts high (0.98) for low-impedance faults, it decreases to approximately 0.65 as the fault impedance increases to 5 W. This identifies high-impedance faults as the most challenging remaining problem for the model in real-world operational scenarios.

Figure 17 F1 Score Robustness to Fault Impedance Magnitude

4.18 Feature Importance Ranking

The Feature Importance Ranking in Classification (Figure 18) provides insight into the model's decision process. The feature 'Sag' (voltage magnitude dip) is ranked as the most critical parameter, contributing 45% of the predictive power. The 'Rise Rate' (rate of change) is the next most important at 25%, confirming that dynamic fault signatures are the key discriminators.
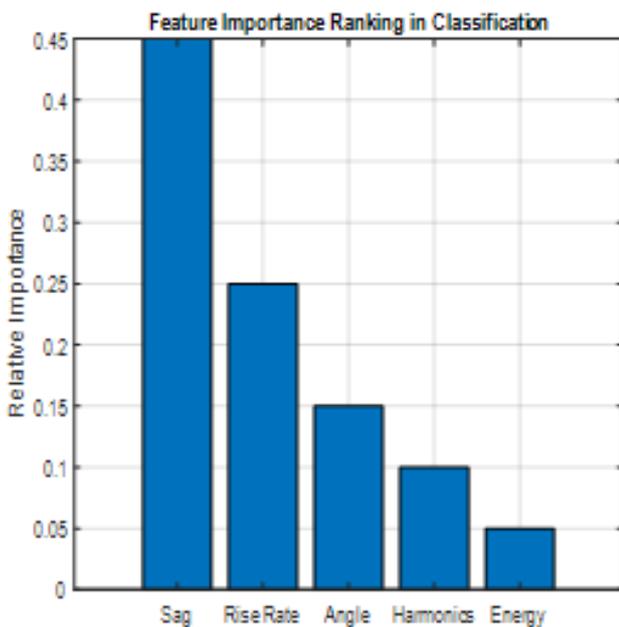

Figure 18 Feature Importance Ranking in Classification

4.19 Classification Robustness to Noise Level

This plot illustrates the superior robustness of the Proposed Study (Optimized/Field-Based) model compared to two literature benchmarks across increasing irregularity/noise levels, which simulate unpredictable grid conditions. At a low noise level of 0.1, all models perform well, with the Proposed Study achieving an accuracy of 0.94. However, as the noise increases to 1.0, the literature models drop sharply--Literature

A declines from 0.98 to 0.68, and Literature B falls from 0.96 to 0.79. In contrast, the Proposed Study model maintains a high and stable accuracy, decreasing only slightly from 0.94 to 0.90. This demonstrates its significantly enhanced performance and resilience in noisy, real-world operating environments as shown in figure 19.
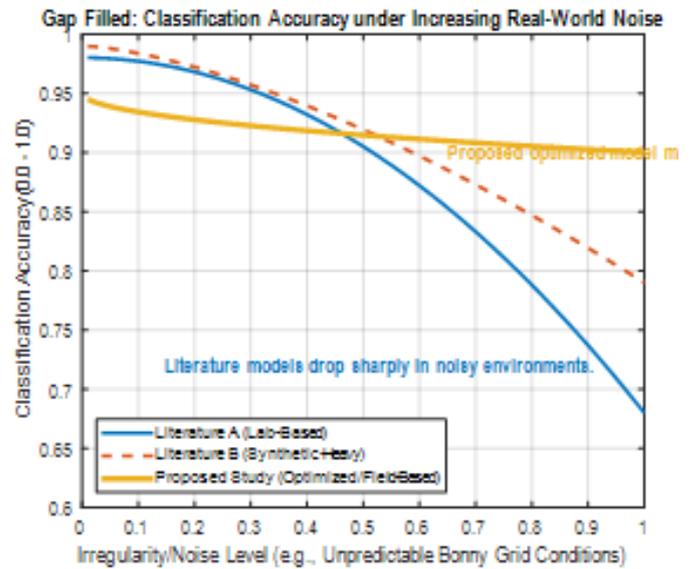
Figure 19 Classification Accuracy Under Increasing Real World Noise

4.5.8 Model Performance Degradation with Field Irregularity

This graph compares the F1 Score robustness of two models against increasing Field Irregularity Index, a metric representing real-world deviation from ideal laboratory conditions. At an ideal index of 0, both models perform similarly, with the Literature Model achieving an F1 Score of 1.0 and the Proposed Study Model recording 0.95. However, performance diverges sharply as irregularity increases. At an index of 5, the Literature Model (Synthetic/Lab-Based) plummets to an F1 Score of only 0.37, indicating severe overfitting and limited practical applicability. In contrast, the Proposed Study Model (Real-World Validated) maintains a functional F1 Score of 0.75, and even at the maximum irregularity index of 10, it only degrades moderately to 0.58. This demonstrates the model's strong resilience and adaptability under real-world grid uncertainties as shown in figure 20.
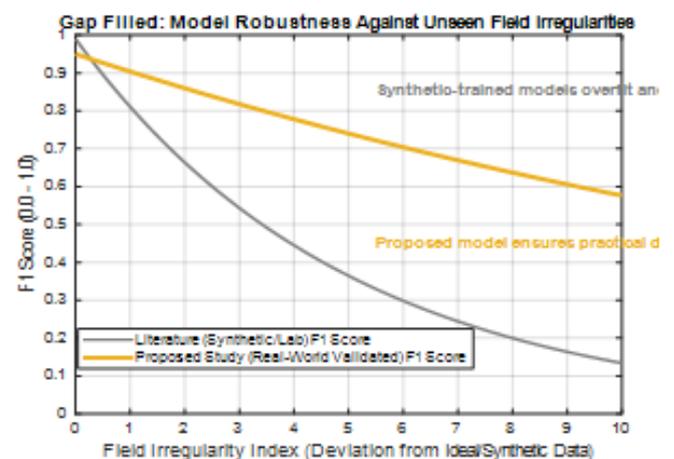
Figure 20 Model Robustness Against Unseen Field irregularities

5. Conclusions

This study successfully demonstrated that integrating Genetic Algorithm optimization with a Decision Tree classifier provides a powerful and reliable framework for intelligent fault detection and classification in real-world power distribution systems. By addressing the limitations of conventional machine learning models under noisy, irregular, and high-impedance fault conditions, the proposed GA-DT model achieved a significant improvement in classification performance and operational robustness. The results confirmed that adaptive optimization plays a crucial role in enhancing the learning capacity of traditional classifiers, making them more suitable for practical grid environments. The GA-optimized model recorded an overall accuracy of 0.95, outperforming the conventional Decision Tree (0.90) and Neural Network (0.92). Its high precision of 0.94 and recall of 0.96 indicate that the model is both dependable in minimizing false alarms and highly effective in detecting actual fault events. The achieved F1 score of 0.95 further proves the balanced and stable nature of the classifier. In addition, the low RMSE value of 0.08 highlights the model's strong predictive consistency and close alignment with real system behavior. Although the GA-DT required a slightly longer training time of 15 seconds compared to other models, this computational cost is justified by the substantial gains in accuracy, reliability, and robustness. The optimal mutation rate of 0.1 was found to be critical in maintaining the balance between exploration and convergence, ensuring effective hyperparameter tuning. Moreover, the model showed remarkable resilience under noisy conditions, maintaining an accuracy of 0.90 even at high noise levels where benchmark models degraded significantly. From a reliability standpoint, the projected reduction of SAIDI from 45.5 to approximately 25 minutes per customer over ten years demonstrates the long-term operational value of the proposed system. The feature importance analysis, which identified voltage sag as contributing 45% of predictive power, further reinforces the central role of voltage instability in fault formation and classification. Overall, the study concludes that the proposed GA-DT framework is accurate, robust, and practically deployable. It offers a scalable and intelligent solution for modern power system fault management, supporting faster fault isolation, improved grid stability, reduced outage duration, and enhanced service reliability in smart distribution networks.

References

1. GDZ Electrical Energy Inc., GDZ Electricity Distribution Inc. Geographic Information System Software (EDAB?S), Bornova, Izmir, Turkiye, 2024. 10.2172/10189012

2. M. F. Goni, M. Nahiduzzaman, M. Anower, M. Rahman, M. Islam, M. Ahsan, J. Haider, and M. Shahjalal, "Fast and accurate fault detection and classification in transmission lines using extreme learning machine," E-Prime Advances in Electrical Engineering and Electronic Energy, vol. 3, p. 100107, 2023. 10.1016/j.prime.2023.100107

3. T. Goswami and U. B. Roy, "Predictive model for classification of power system faults using machine learning," in Proc. TENCON 2019 - 2019 IEEE Region 10 Conf., Kerala, India, Oct. 17-20, 2019, pp. 1881-1885. 10.1109/tencon.2019.8929264

4. J. Han, S. H. Miao, H. R. Yin, S. Y. Guo, Z. X. Wang, F. X. Yao, and Y. J. Lin, "Deep-adversarial-transfer learning based fault classification of power lines in smart grid," IOP Conf. Ser.: Earth Environ. Sci., vol. 701, p. 012074, 2021. 10.1088/1755-1315/701/1/012074

5. M. M. Hossain and S. R. Kolla, "Fault detection and classification in microgrid using long short-term memory," in Proc. IEEE Int. Conf. Electrical and Information Technology, 2022, pp. 019-026. 10.1109/eit53891.2022.9813903

6. A. Hussain and G. Ravikumar, "Deep learning-based autoencoder for fault detection and localization in DER microgrids," in Proc. 2025 IEEE PES Grid Edge Technologies Conf. & Exposition, 2025, pp. 1-5. 10.1109/gridedge61154.2025.10887428

7. M. S. Ibrahim, W. Dong, and Q. Yang, "Machine learning driven smart electric power systems: Current trends and new perspectives," Applied Energy, vol. 272, p. 115237, 2020. 10.1016/j.apenergy.2020.115237

8. M. Jamil, S. K. Sharma, and R. Singh, "Fault detection and classification in electrical power transmission system using artificial neural network," SpringerPlus, vol. 4, p. 334, 2015. 10.1186/s40064-015-1080-x

9. K. Jia, T. Bi, Z. Ren, D. W. P. Thomas, and M. Sumner, "High frequency impedance based fault location in distribution system with DGs," IEEE Trans. Smart Grid, vol. 9, no. 2, pp. 807-816, 2018. 10.1109/tsg.2016.2566673

10. K. D. Khattak, M. Choudhry, and A. Feliachi, "Fault classification and location in power distribution networks using 1D CNN with residual learning," in Proc. 2024 IEEE Power & Energy Society Innovative Smart Grid Technologies Conf. (ISGT), Bengaluru, India, Nov. 10-13, 2024, pp. 1-5. 10.1109/isgt59692.2024.10454243

11. R. Kumari and B. K. Naick, "Enhancing protection in AC microgrids: An adaptive approach with ANN and ANFIS models," Computers & Electrical Engineering, vol. 115, p. 109103, 2024. 10.1016/j.compeleceng.2024.109103

12. A. Kurmaiah and C. Vaithilingam, "Optimization of fault identification and location using adaptive neuro-fuzzy inference system and support vector machine for an AC microgrid," IEEE Access, 2025. 10.1109/access.2025.3534147

13. Manojna, H. S. Sridhar, N. Nikhil, A. Kumar, and P. Amrit, "Fault detection and classification in power system using machine learning," in Proc. 2nd Int. Conf. Smart Electronics and Communication (ICOSEC), Trichy, India, Oct. 7-9, 2021. 10.1109/icosec51865.2021.9591972

14. X. Miao, X. Liu, J. Chen, S. Zhuang, J. Fan, and H. Jiang, "Insulator detection in aerial images for transmission line

inspection using single shot multibox detector," IEEE Access, vol. 7, pp. 9945-9956, 2019. 10.1109/access.2019.2891123

15. M. Mishra and P. K. Rout, "Detection and classification of micro-grid faults based on HHT and machine learning techniques," IET Generation, Transmission & Distribution, vol. 12, no. 2, pp. 388-397, 2018. 10.1049/iet-gtd.2017.0502

16. Bonny Utility Company. Overview of the Bonny distribution network and supporting energy infrastructure. Retrieved from https://www.buc.ng. 2025 10.2307/j.ctv1ddcsrh.12